Reprinted from the Journal of The American Ceramic Society, Vol. 62, No. 1-2 January-February, 1979

Strength Degradation of Glass Impacted with Sharp Particles: I, Annealed Surfaces

S. M. WIEDERHORN*

Fracture and Deformation Division, National Bureau of Standards, Washington, D. C. 20234

B. R. LAWN*

Department of Applied Physics, School of Physics, The University of New South Wales, Kensington, New South Wales 2033, Australia

The strength characteristics of annealed brittle surfaces impacted with sharp particles were studied. A theory of the degradation process is constructed in three steps: (1) A sharp particle delivers an impulsive load to the target surface via a plastic contact; (2) the contact loading initiates and propagates median cracks in the surface; (3) the cracks thus induced reduce the strength of the material. Static indentation tests provide essential contact parameters for the degradation equations, thereby allowing for prediction of strengths under in-service conditions. Strength tests on soda-lime glass laths impacted with SiC grit confirm basic predictions of the theory. Higher toughness and lower hardness are the main material requirements for improved resistance to degradation. Initial flaw population in the target surface and projectile geometry are not important factors in the damage process. The study shows that impact energy is the important service variable in determining the extent of strength loss.

I. Introduction

BRITTLE ceramic materials are highly susceptible to contact-induced surface cracking. Where ceramics are used as structural components (e.g. radomes, ir-transparent windows, and gas turbine blades) the severe surface degradation caused by impact with small dust particles (or even raindrops) can be a prime factor in engineering design. A single contact event can cause a severe reduction in strength of an exposed component; subsequent events may not cause further significant strength loss, but may cumulate as surface damage to produce deleterious erosion effects.

A rationale for placing the study of strength degradation on a sound scientific footing derives from indentation fracture mechanics.[1,2] Based on whether the contact is essentially elastic or plastic, indenting particles are respectively classified as "blunt" or "sharp"; "real" contacts are then seen as falling within these two extreme types. For statically loaded particles, fracture mechanics provides relations between indentation load and crack size. In conjunction with a standard strength equation this leads directly to a strength/load characteristic for a given indenter/specimen system. Then, for impacting particles, specification of the impulsive load delivered as a function of incident velocity allows an analogous strength/velocity characteristic to be determined for a given projectile/target system. This type of indentation fracture approach has been used to analyze blunt/static,[3] sharp/static,[4] and blunt/impact[5] situations; only the sharp/impact case remains to be considered.

The aim of the present study was to complete the blunt/sharp, static/impact dichotomies with an investigation of the strength degradation suffered by glass surfaces as a result of impact with sharp particles. An important feature of the analysis is the a priori prediction of the degradation characteristics, using only parameters obtained in routine static indentation tests. In deriving an expression for load in terms of velocity the equations of plastic contact are used, thereby bringing hardness into the description. The analysis indicates explicitly the material parameters to be optimized in design against potential strength loss.

The present paper (Part I of a two-part study) deals solely with surfaces initially in a stress-free state, i.e. annealed surfaces. One of the most effective means of improving resistance to strength degradation is to put the surfaces into residual compression by tempering[6]; the present analysis is extended to tempered surfaces in Part II.

Received March 10, 1978; revised copy received July 5, 1978.

Supported at the National Bureau of Standards by the Office of Naval Research, Metallurgy and Ceramics Program, and at the University of New South Wales by the Australian Research Grants Committee.

*Member, the American Ceramic Society.

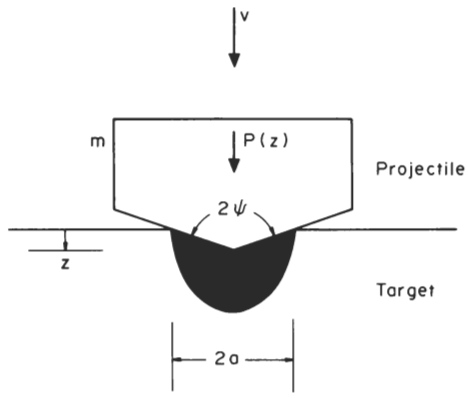

Fig. 1. Parameters of idealized projectile/target system. *Shaded area* designates plastic contact zone.

II. Prediction of Strength/Velocity Characteristic

The distinguishing feature of a sharp-indenter fracture pattern is the controlling role of deformation processes in events close to the contact site. Beneath the point of a sharp indenter, plastic flow (or, in some glasses or other ceramics, viscous flow or structural densification) operates, thereby removing a stress singularity in an otherwise elastic field about the indenter point.[7,8] The localized deformation micromechanics determines the intensity of the indentation stress field and provides nucleation centers for the resultant contact cracks. In the present analysis equilibrium conditions will be assumed throughout.

(1) Impulsive Load Delivered by Impacting Sharp Particle

The first step in the formulation is to determine the maximum impulsive load, P_m, delivered to the target surface by the impacting particle velocity, v. It is assumed here that the contact velocity is slow relative to sonic velocities in either the target or projectile materials, i.e. that quasi-static conditions prevail throughout the contact (the complexity of truly dynamic impact situations is beyond the scope of this work[9]). It is also assumed that the indenting particle strikes the target surface at normal incidence such that the equations of motion contain no rotational component. Generally, calculations based on these assumptions would be expected to overestimate the impulsive load.

An idealized representation of the sharp-indenter contact configuration is shown in Fig. 1. The indenting particle, mass m and characteristic included angle 2ψ, is assumed to be perfectly rigid and to maintain its shape during penetration. It exerts on the target surface a load $P(z)$, where z is the penetration depth. Within the bounds of the quasi-static approximation, the load at any stage of the contact may be expressed in terms of the mean indentation pressure

$$p_0 = P/\Lambda\pi a^2 \equiv H \tag{1}$$

where a is a surface dimension of the plastic impression and Λ is a geometrical factor (e.g. for a cone indenter where a is the impres-

sion radius, $\Lambda=1$, and for a pyramid indenter where a is the impression half-diagonal, $\Lambda=2/\pi$). In the event of geometrical similarity, at all P, for a given indenter, the mean contact pressure identifies with the hardness H,[10] which characterizes the deformation properties of the target surface. In Eq. (1) the hardness is taken to be a material constant, although in most brittle solids it does depend somewhat on load rate, especially at low loads (typically, at $P<1$ N).[11,12] Noting from Fig. 1 that

$$a=z\tan\psi \tag{2}$$

the load/penetration function is obtained:

$$P(z)=(\Lambda\pi H\tan^2\psi)z^2 \tag{3}$$

Now the work done by the penetrating particle in creating the plastic impression is given by

$$W_p=\int_0^{z_m}P(z)\,dz \tag{4}$$

where z_m is the maximum penetration. In combination with Eq. (3) this gives

$$W_p=P_m{}^{3/2}/(9\Lambda\pi H\tan^2\psi)^{1/2} \tag{5}$$

where P_m is the load at maximum impression. On the assumption that all the kinetic energy of the impinging particle

$$U_K={}^1/_2 mv^2 \tag{6}$$

is dissipated in the irreversible plasticity processes, i.e. that $U_K=W_P$, we have

$$P_m=(9\Lambda\pi H\tan^2\psi)^{1/3}U_K{}^{2/3}=(2.25\Lambda\pi Hm^2\tan^2\psi)^{1/3}v^{4/3} \tag{7}$$

In general, not all the incident kinetic energy will be expended as plastic work, in which case the particle will rebound. Thus Eq. (7) represents an upper bound to the impulsive load.

It is of interest to compare the functional form of Eq. (7) for sharp indenters, $P_m=P_m(H,m,\psi,v)$, with the analogous equation for blunt indenters,[5] $P_m=P_m(E,m,r,v)$ (E = Young's modulus, r = indenter tip radius); in the context of material properties, it is stiffness which determines the load response in impacts with blunt indenters, whereas with sharp indenters it is hardness which controls.

(2) Indentation Fracture Relations

The evolution of indentation cracks in the sharp-contact stress field is complex.[2,7,8,13] The present paper deals only with those essential features which are pertinent to the strength degradation question. As it penetrates the target surface, the indenter sets up a concentration of tensile stress at the base of the elastic/plastic zone interface. Although increasing the load does not increase the *intensity* of the tensile stress field, which is controlled by the constant contact pressure (Eq. (1)), it does increase the *spatial extent* of the field. Accordingly, at some critical load, P_c, a favorably situated subsurface flaw will experience tension over a sufficient portion of its area that an instability in the crack size occurs[13]:

$$P_c=\alpha_P K_c{}^4/H^3 \tag{8}$$

where α_P is an elastic/plastic geometrical factor, to be determined empirically for a given indenter/target system, and K_c is the toughness of the target material. The validity of this derivation rests with the availability of a suitable starting flaw, either deformation-nucleated or preexistent, and thereby represents a minimum threshold condition for crack initiation. Equating P_c in Eq. (8) to P_m in Eq. (7) gives a conservative basis for calculating critical impact velocities corresponding to the onset of strength loss. However, in many brittle ceramics (e.g. the glass in the present study) v_c is so low that newly formed indentation cracks are lost in the "noise" of preexisting centers; in such cases we may conveniently take the threshold as effectively zero.

Once formed, the indentation cracks develop as expanding half-pennies centered about the contact point and normal to the surface; the half-pennies usually orient along certain symmetry planes, e.g. the diagonals of pyramid impressions.[2,8] These are the median cracks which are primarily responsible for any ensuing strength degradation. Application of Griffith/Irwin fracture mechanics provides the following relation for the crack depth D in terms of indentation load,[8]

$$P/D^{3/2}=\beta_P K_c \qquad (P>P_c) \tag{9}$$

where β_P is another geometrical factor, calculated as $\approx\pi^{3/2}\tan\psi$ but again usually determined empirically for a given indenter/target system. The crack depth may now be expressed in terms of impact velocity by equating P in Eq. (9) to P_m in Eq. (7).

Median cracking is only part of the indentation fracture picture. When specimens are unloaded, sideways-extending, "lateral" cracks initiate from the plastic zone and grow toward the specimen surface.[7] Although important in erosion, these cracks do not contribute directly to strength degradation and need not be given explicit attention here.

In comparison with the fracture mechanics of blunt indenters, the present formulation differs significantly in the initiation equation, but not in the propagation equation[2,5]; in severe contact conditions the fracture mechanics are relatively insensitive to indentation geometry.

(3) Strength Characteristics

The standard form of the equation for the tensile strength of brittle solids is

$$\sigma=K_c/(\pi c_f)^{1/2} \tag{10}$$

where c_f is the effective length of the dominant flaw. In impact with particles of given mass, there will exist some "cutoff" velocity v^* below which preexistent centers dominate and above which the indentation cracks dominate. That is,

$$c_f=c_{f0} \qquad (v<v^*) \tag{11a}$$

$$c_f=\Omega D \qquad (v>v^*) \tag{11b}$$

where c_{f0} is the characteristic size of preexisting flaws and $\Omega=4/\pi^2$ for ideal penny cracks.[4] The cutoff is determined either by the threshold velocity v_c, at which full-scale median cracking initiates, or by the crossover velocity v' at which the condition $\Omega D=c_{f0}$ is satisfied, whichever of the two is the greater.[2]

The required strength degradation characteristics are now obtained by eliminating crack length and indentation load from Eqs. (7) to (11):

$$\sigma=K_c/(\pi c_{f0})^{1/2} \qquad (U_K<U_K{}^*) \tag{12a}$$

$$\sigma=[(1/9\pi^{5.5})^{1/9}(\beta_P{}^3/\Lambda\tan^2\psi)^{1/9}(K_c{}^{4/3}/\Omega^{1/2}H^{1/9})]\,U_K{}^{-2/9} \qquad (U_K>U_K{}^*) \tag{12b}$$

III. Impact Damage and Contact Parameters

(1) Impact Apparatus and Test Procedure

The equipment used to produce the impact damage is described in detail elsewhere.[14] Particles are gravity-fed from a hopper into a gas stream and accelerated through a tungsten carbide nozzle onto the target surface. Incident particle velocities are calibrated by a rotating disk method: two disks, the first containing a narrow slit, rotate in unison about an axis common with the direction of particle flow, the angular displacement of abrasion marks left on the second disk relative to the slit position providing the velocity measurement.[15] With this apparatus, velocities of 10 to 120 m s^{-1}, with an accuracy of $\approx$ 10%, are attainable.[14] Velocities <10 m s^{-1} are most easily achieved by free fall down a vertical glass tube.

The main source of projectiles for the present study was sieved SiC grit (Table I). Individual SiC particles are hard and angular

Table I. Projectile Masses

Material	Density (Mg/m^3)	Mesh size	Sieve opening (μm)	Mass (μg)
SiC (carborundum grit)	3.2	30	590	345
		60	250	26
		100	150	5.6
		200	75	0.68
SiO_2 (glass beads)	2.5	35	500	165

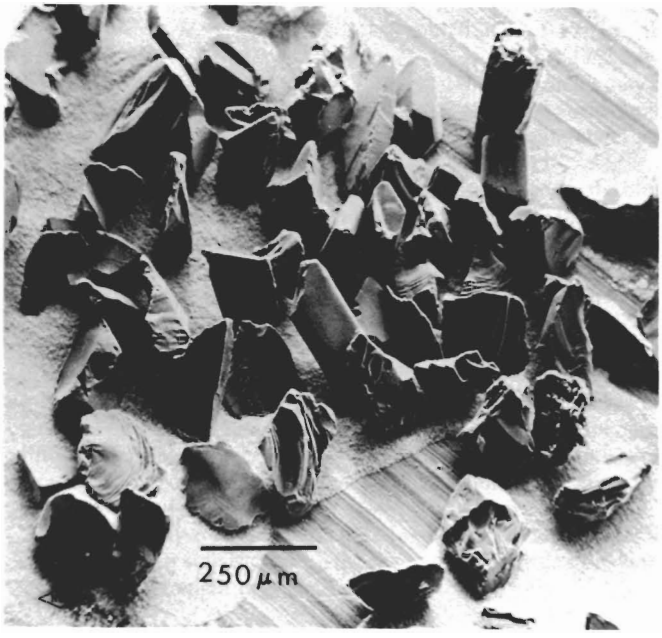

Fig. 2. Scanning electron micrograph of 100-mesh SiC particles used in degradation tests (courtesy E. R. Fuller and B. J. Hockey).

Table II. Sieve Analysis of Abrasives Used in the Strength Degradation Studies

Mesh	Sieve size*	% Retained	Mesh	Sieve size	% Retained
30	25	6	100	100	36
	30	59		120	31
	35	34		140	20
	40	1		200	11
	Fines	0		Fines	2
60	50	11	200	170	14
	60	48		200	33
	70	32		230	9
	80	8		270	26
	Fines	1		Fines	18

*All sieve sizes quoted are U.S.A. standard screen sizes (ASTM Standard E11-70).

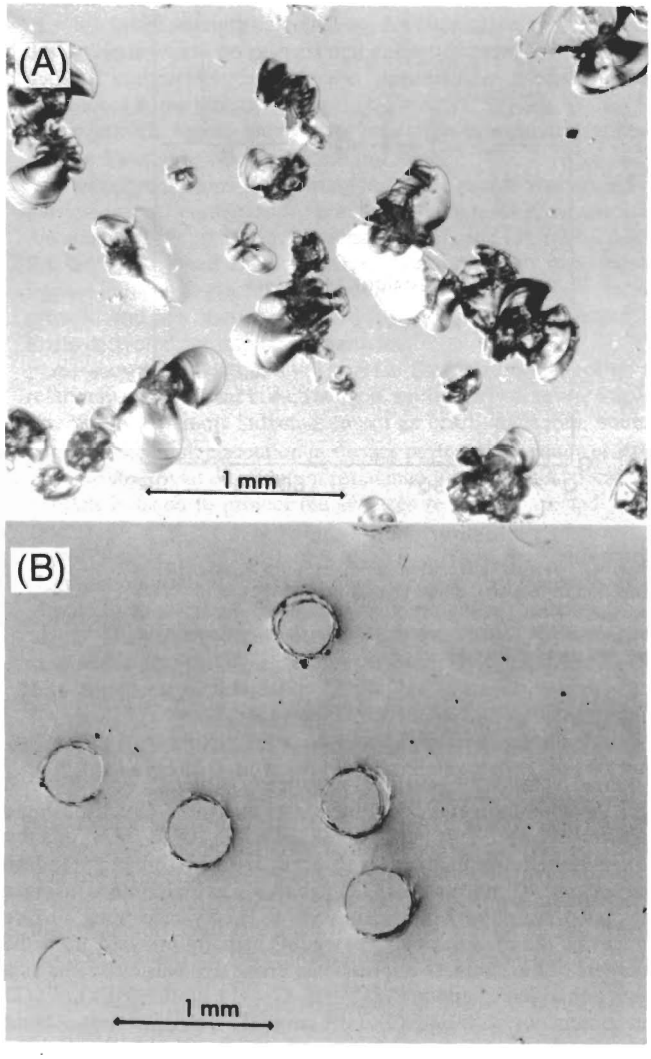

Fig. 3. Optical micrographs of soda-lime glass surfaces impacted with (*A*) 100-mesh SiC particles, velocity 113 m s^{-1} and (*B*) 35-mesh glass beads, velocity 102 m s^{-1}

(Fig. 2) and thus convenient for simulating sharp-indenter conditions; however, close examination of edges and corners on $\approx 5\ \mu m$ scale did show some tendency to rounding. A sieve analysis of the four mesh sizes that were used is given in Table II. Particle masses were calculated on the basis that the opening of the sieve grid determines the diameter of an equivalent spherical particle. To ensure that no particles larger than those indicated in Table I impacted on the target surface, the particles used in the grit-blast experiments were passed through sieves of the nominal mesh size before use. Some comparison tests were also run with glass bead projectiles of 35 mesh, to typify blunt-indenter conditions. The number of particles fed into the impact apparatus was always kept small enough that mutual interactions between contact sites were minimized at the target surface.

For the target, soda-lime glass laths of the same type as described in previous studies ($\approx$250 by 37.5 by 5.65 mm)[3–5] were used. The as-received laths were first acid-polished to remove edge flaws, so that any ensuing contact damage provided the dominant flaw over the operative range of impact velocities. Particle impact was confined to a small central area on one face of each lath, and this area was covered with mineral oil immediately after exposure to the particle beam to minimize moisture-assisted kinetic effects in the subsequent fracture tests. Strength was then measured in four-point bending (major span 204 mm, minor span 37.5 mm), with the impacted face of the lath on the tension side.[3–5] Control tests on 14 unimpacted surfaces (also acid-polished) gave a mean and standard deviation in strength of (174±72)MPa; here edge failures were unavoidable and were the main contributor to the base level in strength.

(2) Damage Morphology

The damage morphology produced on the glass surfaces by the SiC and glass projectiles showed all the classical features of quasi-static sharp/blunt indenter patterns,[1,2] with the only obvious variants due to geometrical variations in the particles themselves (Fig. 2). Figure 3 shows typical damage morphology. With the sharp SiC particles (Fig. 3(*A*)) the most conspicuous damage is the surface spalling attributable to the lateral cracks. Also evident as fine radial traces on the surface (sometimes forming confining boundaries for the chipped regions) are the median cracks primarily responsible for the strength degradation. A more detailed correspondence between quasi-static indentation and particle impact damage is currently under investigation and is to be reported elsewhere.[16,17] With the glass beads (Fig. 3(*B*)) the characteristic circular trace of the Hertzian cone type fracture, typical of blunt indenter patterns, is apparent. In each of the micrographs the relative scale of neighboring damage patterns gives some indication of the uniformity of the impact conditions for any given particle beam.

(3) Contact Parameters

Applying Eqs. (12) to prediction of strength degradation requires knowledge of contact parameters for a given indenter/specimen system. These parameters are readily obtained from standard indentation tests, coupled with some control bend tests.

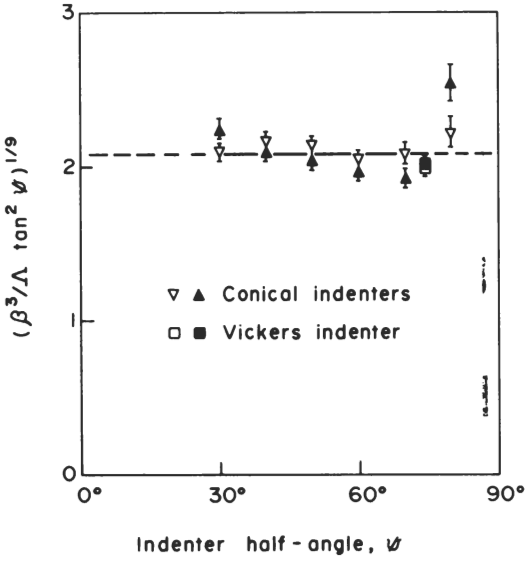

Fig. 4. Plot of indentation geometry term in Eq. (12) as function of indenter angle. Data from Ref. 8; median crack results with penny radius measured from both surface traces (filled symbols) and depth measurements in profile (open symbols).

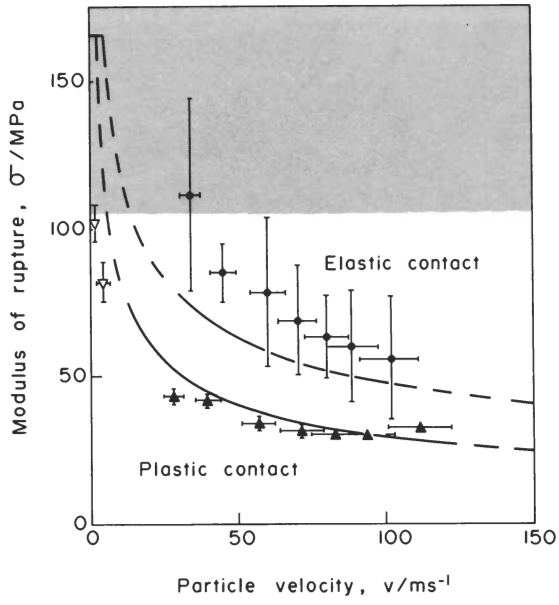

First, values of the material parameters H and K_c were obtained for the soda-lime glass. Hardness was measured directly using a Vickers pyramid indenter, over a load range 10^0 to 10^2N, in a dry nitrogen environment: $H=(5.5\pm0.2)$ GPa (mean±standard deviation, 40 indentations). Toughness was determined using a two-step procedure outlined in Ref. 6: (1) By measuring surface traces of the median cracks extending radially outward from the corners of the hardness impressions, crack size was evaluated as a function of load,[8] giving $P/D^{3/2}=\beta_P K_c=(11.5\pm0.4)$MPa m$^{1/2}$; (2) in conjunction with Eqs. (9), (10), and (11*b*), a run of control bend tests on Vickers-indented laths gave $\sigma P^{1/3}=(\beta_p K_c^4)^{1/3}/(\pi\Omega)^{1/2}=(140\pm10)$MPa N$^{1/3}$ (40 specimens). With $\Omega=4/\pi^2$, combining (1) and (2) yields $K_c=(0.70\pm0.06)$MPa m$^{1/2}$.

Next, the geometrical terms β_p, Λ, and ψ in Eq. (12) were investigated. For a Vickers pyramid, $\Lambda=2/\pi$, $\psi=74°$ (angle between opposing edges), and $\beta_P=16.4\pm1.9$ from the above data. However, for the SiC of prime interest here, it is clear from Fig. 2 that the prospective contacting points of the particles embrace a wide range of indentation geometries. On the other hand, from the definition of the terms in Eq. (9), $\beta_p \propto \tan\psi$ approximately, so that the composite term $(\beta_p{}^3/\Lambda \tan^2\psi)^{1/9}$ which appears in Eq. (12) is expected to be a slowly varying function of ψ. This result is demonstrated in Fig. 4, in which the value of this term for the Vickers indentations is compared with data from conical indenters covering a range of included angles.[8] The geometrical insensitivity of this plot allows us to regard all sharp indenter points as "equivalent Vickers pyramids," for which $(\beta_p{}^3/\Lambda \tan^2\psi)^{1/9}=2.02\pm0.08$.

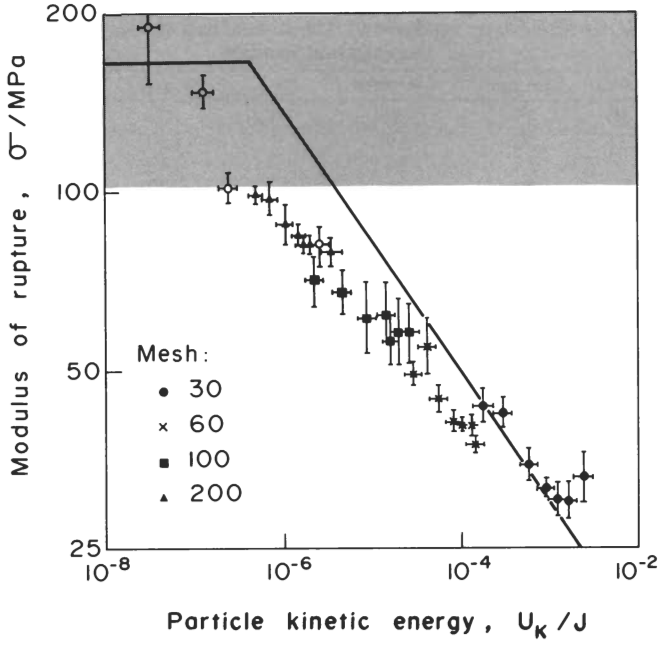

Fig. 6. Strength degradation of soda-lime glass impacted with SiC grit particles, plotted as function of particle energy (open symbols designate free-fall data). *Shading* designates standard deviation limits of strengths for unimpacted laths (acid-polished).

IV. Strength Degradation Results

To investigate the main features of the degradation theory of Section II, series of impact/strength tests were run as a function of velocity for each of the particle types. For each series with SiC particles an appropriate function $\sigma(v)$ (using Eq. (6)) or $\sigma(U_K)$ was generated from Eq. (12) using the parameters determined in Section III(3). The corresponding function for glass beads was generated from the analogous blunt-indenter relation Eq. (7) in Ref. 7. Theoretical predictions (solid lines) and experimental results (data points, each representing mean±standard deviation, four tests), are compared in Figs. 5 and 6. In these plots low-velocity (or low-energy) impact, in which the strength is controlled by preexisting surface flaws, may be distinguished from high-energy impact, where the strength is indentation-controlled. Under the present impact conditions, the existence of any threshold in the indentation fracture is lost in the noise.

Basically, in addition to the velocity dependence, the tests examined the effects of shape and size of the particles.

(1) Effect of Particle Shape and Flaw Availability

The first tests were conducted to determine the influence of particle shape on the degradation characteristics. The results are shown in Fig. 5, as a comparison between blunt and sharp indenting particles of similar size. Two important features are:

(1) Sharp particles have greater capacity than blunt particles to degrade the surface. Table I shows that the 35-mesh glass beads

have half the mass of the 30 SiC particles; however, since $\sigma \propto m^{-2/9}$ in Eq. (12*b*), σ(35-mesh glass)/σ(30-mesh SiC)$\approx$1.17, i.e. the factor of two in masses accounts for a difference of only 17% in the strength curves. The greater degradation with sharp particles may be attributed to the greater penetration and more favorable orientation of the medians as compared to the cones in the indentation cracking.[5]

(2) The scatter in data is much less for the sharp than for the blunt indenters. This scatter reflects an important difference in the initiation of the indentation cracks; in particular, the question of flaw availability arises. With blunt indenters the indentation prior to cone cracking is elastic, and the expanding contact area has to search for a suitable starting fracture nucleus on the target surface.[1,2] Such nuclei are not abundant on the acid-polished glass surfaces, hence the scatter.[5] With sharp indenters, however, the indentation is plastic, and the deformation processes within the plastic zone are capable of producing their own incipient flaws.[4] There is therefore little to be gained by producing ultra-high-quality surface finishes in ceramic components exposed to particles with sharp corners or edges.

The relatively small scatter in the $\sigma(v)$ data for the sharp particles in Fig. 5 is also consistent with the expected minor role of indenter angle in the strength degradation (Fig. 4).

(2) Effect of Particle Size

The major part of the test program concentrated on the degradation characteristics for the four SiC particle mesh sizes listed in Table I. With these results both the mass and velocity dependence of the strength can be accommodated on a single, "universal" $\sigma(U_K)$ plot. Figure 6 compares the data with the theoretical prediction of Eq. (12). Agreement between predicted and observed results is obtained, within the limits of scatter, over a greater part of the energy range studied, although there does appear to be a systematic tendency for the data points to cross above the theoretical line in going from lower to higher energies. Some possible origins of this tendency are discussed in some detail elsewhere,[5] especially in terms of dynamic effects (e.g. diminished contact times), stress relief due to crushing and multiple cracking at the impact site, etc; another possible origin, in terms of variations in the particle shape, is discussed below.

V. Discussion

The preceding sharp-particle analysis of degradation has certain implications in the engineering design of ceramics for structural applications. Given routine mechanical testing facilities for determining appropriate indentation constants, the formulation opens the way to simple strength predictions for seemingly complex projectile/target systems. As with the complementary analysis for blunt indenters,[5] the important variables appear in the degradation equations in simple power form; system optimization then becomes, in principle, a straightforward process of material selection.

Thus, in choosing a suitable target material for a particular application, the strength should be maximized in accordance with the prospective particle mass and velocity. The most conservative basis for design is the presumption that indentation fracture is inevitable; the aim is then to optimize against crack *propagation*, i.e. to maximize the strength, $\sigma \propto K_c^{4/3} H^{-1/9}$ ($U_K > U_K^*$), in Eq. (12*b*). Toughness K_c is clearly the dominant parameter here, and, as expected, should be large to minimize crack growth. Hardness H enters in a much less sensitive way; indeed, it is because of this insensitivity that hardness values obtained statically (Section III(3)) are considered adequate for predicting impact strengths in Eq. (12*b*), typical differences of up to a factor of two in static and dynamic determinations[12] (Section II(1)) corresponding to an error of $<8\%$ in the strength calculations. An alternative, more stringent design basis would be to insist that impact-induced degradation be avoided completely; in this case, optimization is against crack initiation, i.e. the threshold energy, $U_K^* \propto K_c^6 H^{-9/2}$, Eqs. (7) and (8), is maximized. Again, the primary requirement is maximization of K_c, the secondary is minimization of H.

These conclusions concerning material parameters in sharp-particle impact parallel those previously drawn for blunt particles: the analogous degradation relations (Eqs. (7) and (3) in Ref. 5) call for large K_c, small E. In general, therefore, high resistance to impact-induced degradation implies high toughness, to restrict crack growth, and low hardness and stiffness, to restrict the impulsive loads delivered by impinging particles.

As shown in Section IV(1), prior flaw size and density are relatively insignificant in degradation, particularly at severe impact. The ability of sharp indenters to act as crack-nucleation sources suggests that high perfection in surface preparation is not a practical route to improved degradation resistance, unless some special precaution is taken to protect the surfaces (e.g. as in coated optical fibers).

For a given projectile/target material system the sharp-particle degradation relation Eq. (12*b*) may be conveniently reduced to the simple form $\sigma \propto S U_K^{-2/9}$, where S is a projectile geometry ("size/shape") factor; it has been shown (Fig. 4) that $S \propto (\beta_p^3/\Lambda \tan^2 \psi)^{1/9}$ is reasonably constant over indenter angle ψ. The corresponding relation for blunt particles (Eq. (7) in Ref. 5) reduces similarly to $\sigma \propto S U_K^{-1/5}$, where S is now $\propto r^{-1/15}$. With the SiC particles shown in Fig. 2 it is possible that the observed fine-scale rounding of edges and corners could significantly influence the shape factor for small impressions, thereby explaining the systematic departures of the degradation data from the predicted curve in Fig. 6. Thus, notwithstanding a slow variation in the function S, it may be asserted that the prospective degradation of any projectile/target system is primarily determined by the impact energy, giving some credence to the commonly held empirical notion that general impact damage phenomena may be described in terms of energy criteria.

Acknowledgments: The writers thank B. J. Hockey, G. Garrett, and D. B. Marshall for extensive discussions and for experimental assistance.

References

[1] B. R. Lawn and T. R. Wilshaw, "Indentation Fracture: Principles and Applications," *J. Mater. Sci.*, **10** [6] 1049–81 (1975).
[2] B. R. Lawn and D. B. Marshall; pp. 205–29 in Fracture Mechanics of Ceramics, Vol. 3. Edited by R. C. Bradt, D. P. H. Hasselman, and F. F. Lange. Plenum, New York, 1978.
[3] B. R. Lawn, S. M. Wiederhorn, and H. H. Johnson, "Strength Degradation of Brittle Surfaces: Blunt Indenters," *J. Am. Ceram. Soc.*, **58** [9–10] 428–32 (1975).
[4] B. R. Lawn, E. R. Fuller, and S. M. Wiederhorn, "Strength Degradation of Brittle Surfaces: Sharp Indenters," *ibid.*, **59** [5–6] 193–97 (1976).
[5] S. M. Wiederhorn and B. R. Lawn, "Strength Degradation of Glass Resulting from Impact with Spheres," *ibid.*, **60** [9–10] 451–58 (1977).
[6] D. B. Marshall and B. R. Lawn, "Strength Degradation of Thermally Tempered Glass Plates," *ibid.*, **61** [1–2] 21–27 (1978).
[7] B. R. Lawn and M. V. Swain, "Microfracture Beneath Point Indentations in Brittle Solids," *J. Mater. Sci.*, **10** [1] 113–22 (1975).
[8] B. R. Lawn and E. R. Fuller, "Equilibrium Penny-Like Cracks in Indentation Fracture," *ibid.*, [12] 2016–24.
[9] A. G. Evans and T. R. Wilshaw, "Dynamic Solid Particle Damage in Brittle Materials: An Appraisal," *ibid.*, **12** [1] 97–116 (1977).
[10] D. Tabor, Hardness of Metals. Clarendon, Oxford, England, 1951.
[11] R. E. Hanneman and J. H. Westbrook, "Effects of Adsorption on the Indentation Deformation of Nonmetallic Solids," *Philos. Mag.*, **18** [151] 73–88 (1968).
[12] S. P. Gunasekera and D. G. Holloway, "Effect of Loading Time and Environment on the Indentation Hardness of Glass," *Phys. Chem. Glasses*, **14** [2] 45–52 (1973).
[13] B. R. Lawn and A. G. Evans, "A Model for Crack Initiation in Elastic/Plastic Indentation Fields," *J. Mater. Sci.*, **12** [11] 2195–99 (1977).
[14] S. M. Wiederhorn and D. E. Roberts, "A Technique to Investigate High Temperature Erosion of Refractories," *Am. Ceram. Soc. Bull.*, **55** [2] 185–89 (1976).
[15] A. W. Ruff and L. K. Ives, "Measurement of Solid Particle Velocity in Erosive Wear," *Wear*, **35** [1] 195–99 (1975).
[16] B. J. Hockey, S. M. Wiederhorn, and H. H. Johnson; pp. 379–402 in Ref. 2.
[17] B. J. Hockey; unpublished work.